Radiation damage of $RbMgF_3$†

N. Koumvakalis and W. A. Sibley
Physics Department, Oklahoma State University, Stillwater, Oklahoma 74074
(Received 16 December 1975)

Radiation-induced defects in $RbMgF_3$ have been studied by optical techniques. A tentative identification of the absorption and emission bands associated with these defects suggests the following optical bands occur when the defects designated below are present: (a) $[X_2^-]$ (V_k) centers—330-nm absorption and 428-nm emission, (b) F centers—295- and 325-nm absorption (depends on crystal orientation), (c) F_2 centers—387-, 285-, and 230-nm absorption; 430-nm emission, and (d) F_3 centers—300-nm absorption; and 330- and 490-nm emission. The temperature dependence of the production and annihilation of these defects is also investigated.

I. INTRODUCTION

Radiation damage has been investigated in a number of fluoride crystals[1–7]; however, $RbMgF_3$ has not yet to our knowledge been studied. This material forms as a crystal of hexagonal symmetry with the c axis as the optic axis. All Mg^{2+} ions are in sites of octahedral symmetry surrounded by six fluorine ions, but this complex of MgF_6 ions can have two different orientations in the crystal.[8,9] Figure 1 illustrates the crystal structure. $\vec{a}_1$, $\vec{a}_2$, and $\vec{a}_3$ are unit vectors in the basal plane which contains the seven Rb^+ ions shown. The heavy line denotes the optic axis. Note that the right-hand figure shows three layers of ions (the three Mg^{2+} ions comprise the second layer).

From the considerable amount of work already published on related fluorine compounds such as $KMgF_3$, MgF_2, and the alkali halides[10,11] it is expected that photochemical processes occur with the concomitant formation of vacancies and interstitials. This suggests that γ rays and electrons impinging upon the sample should cause a number of vacancy-interstitial pairs to be formed. It has been shown that the $[X_2^-]$ (V_K) center is a precursor to photochemical damage in highly ionic materials[11] and in order to establish the damage mechanisms operating in this material the identification of $[X_2^-]$, F, F_2 (M), and $F_3(R)$ centers must be established. Thus, the purpose of this paper is to tentatively identify the optical absorption and emission bands which result from the presence of the above defects and to investigate the temperature dependence of radiation damage in $RbMgF_3$.

II. EXPERIMENTAL PROCEDURE

The crystals were grown by the Stockbarger method in an argon atmosphere with crystal chips of MgF_2 and zone-refined RbF as starting material. Graphite crucibles were used. The highest furnace temperature was 890 °C and the growth rate was controlled at 1.5 mm/h. Chemical analysis of one of the crystals was done with mass spectroscopy. The results are shown in Table I. The optic axis of the crystal was determined with a polarizing microscope and the crystal structure was confirmed by Laue x-ray scattering. A diamond saw was used to cut samples with faces perpendicular to the optic axis, $c_\perp$, and parallel to the optic axis, $c_\parallel$. The specimens were irradiated with ^{60}Co γ rays or 1.5-MeV electrons after they had been optically polished. The electron irradiation intensity was measured to be about 1.3×10^{12} e/cm^2sec by means of silver-doped phosphate glass dosimeters. The samples were irradiated and measured in a cryogenerator capable of reaching 10 K with a temperature control of ±1 K. However, the thermocouple measures the temperature just above the sample and it is certain that during irradiation the sample is warmer than 10 K. Optical measurements were made with a Cary 14 spectrophotometer and a 1 m Jarrell-Ash monochromator with associated electronics for both luminescence and double beam absorption detection. Excitation spectra were taken using exciting light from a xenon lamp chopped at 135 Hz and passed through a Spex 22-cm monochromator. The system was calibrated using a standard lamp and all

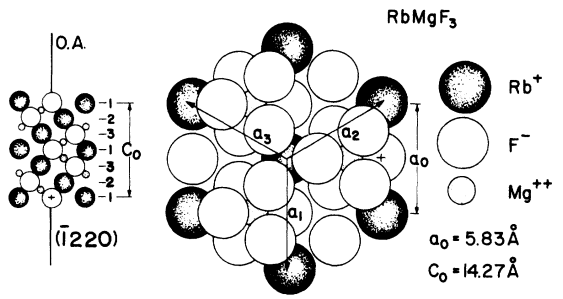

FIG. 1. $RbMgF_3$ model. Shown are the basal plane (three layers with 7 Rb^+ ions, and 12 F^- ions in the first layer and 3 Mg^{2+} ions in the second) and the close-packed sequence of ions along the optic axis which lie in the $(\bar{1}220)$ plane.

Table I. Impurity analysis of $RbMgF_3$ (in ppm).

Ag	~1	Cu	10	Pb	< 25
Al	1075	Fe	100	Pt	< 50
Au	< 5	Ga	< 3	Sb	< 100
B	75	Ge	< 5	Si	60
Ba	2400	Hg	< 100	Sn	< 10
Be	< 20	K	1700	Sr	~ 50
Bi	< 4	Li	120	Ta	< 100
Ca	1040	Mn	< 10	Ti	~ 150
Cd	< 30	Mo	< 5	V	< 40
Co	< 75	Na	540	W	< 50
Cr	< 6	Nb	< 10	Zn	< 50
Cs	< 30	Ni	< 10	Zr	< 50

data were corrected for excitation intensity and system response. Polarized light was needed for a number of the measurements and the light was polarized using Glan polarizers or polaroid type HNP'B ultraviolet sheets. In the case of defect annealing experiments the samples were held for 10 min (in one case when a very large sample was used it was held for 15 min) at the desired temperature and then air cooled to room temperature.

III. RESULTS

Although more evidence must be accumulated before definitive assignment of the defects responsible for the observed optical transitions in irradiated $RbMgF_3$ can be made, there is sufficient evidence at this time to tentatively identify the optical properties of $[X_2^-]$, F_2, and F_3 centers. We will therefore discuss the results in terms of these centers and hope that the information presented here will facilitate the EPR experiments which must be done for the final positive identifications.

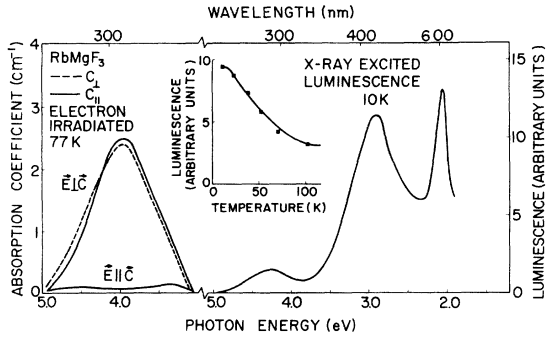

FIG. 2. $X_2^-(V_K)$ absorption at 77 K and x-ray excited luminescence at 10 K. Absorption spectrum is plotted for different electric vector, $\vec{E}$; polarization and orientations, $c_\parallel$ and $c_\perp$, of the optic axis. Inset shows the temperature dependence of the x-ray excited luminescence. (c_j indicates that the c axis is perpendicular to the crystal face.)

A. $[X_2^-]$ centers

Figure 2 portrays the 77-K radiation-induced absorption in $RbMgF_3$ crystals cut with $c_\parallel$ and $c_\perp$. Note that when the electric vector of the incident light is oriented along the optic or c axis, $\vec{E} \parallel \vec{C}$, no absorption is evident at 330 nm (3.75 eV) in samples irradiated for 30 sec to 1 min. However, for the electric vector perpendicular to the optic axis, $\vec{E} \perp \vec{C}$, an absorption band is evident. The magnitude of this absorption remains constant after only a few seconds of irradiation. In irradiated crystals no dichroism of the 330-nm band is observed when light is propagating along the optic axis; however, the band can be made dichroic by exposing the sample to polarized 330-nm light for 1 h. It was found that the absorption which was polarized in the same way as the bleaching light was decreased.

The x-ray excited emission is also portrayed in Fig. 2 as is the temperature dependence of this emission. Emission bands are present at 288 nm (4.3 eV); 428 nm (2.9 eV); and 600 nm (2.05 eV). The use of a filter to cut off all emitted light with energy greater than 3.4 eV shows that although there is some second-order contribution at 600 nm from the 288-nm emission band there is a 600-nm band. The thermal annealing of the 330-nm band is shown in Fig. 3. The curves are drawn from data taken on $c_\perp$ samples which were bleached with polarized light. The bleaching directions are indicated on the figure. It might be expected that if the absorption is polarized the emission should also exhibit this effect. However, no polarization of the x-ray excited emission could be detected. It was not possible to measure the optically excited emission from this defect since the concentration of defects was small and was reduced rapidly by the bleaching light. A comparison of the positions of the absorption and emission of these bands in $RbMgF_3$ and their saturation with irradiation and

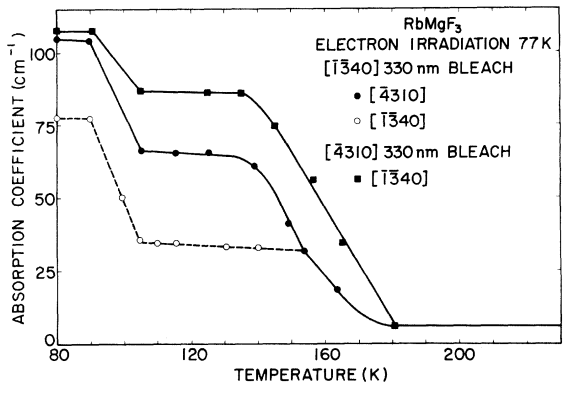

FIG. 3. Thermal annealing curves of the V_K absorption for different bleaching directions.

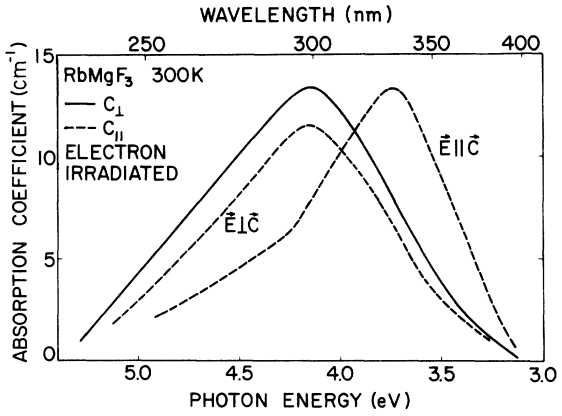

FIG. 4. E-center absorption spectra for different $\vec{E}$ polarizations and orientations, $c_{\parallel}$ and $c_{\perp}$, of the c axis.

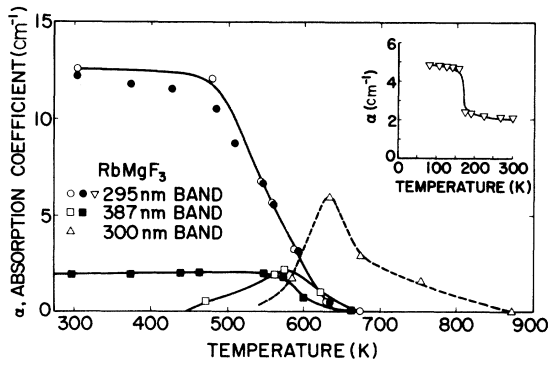

FIG. 6. Thermal annealing curves for F, F_2, and F_3 centers. Inset shows the annealing behavior of the F center at low temperatures for a *light* dose (10^{15} MeV/cm^3) of irradiation. Full squares represent data on a sample irradiated at 550 K.

thermal annealing characteristics with those in[7] $KMgF_3$ and[6] $KZnF_3$ suggests that the bands are due to $[X_2^-]$ centers.

B. F centers

When $RbMgF_3$ is irradiated at temperatures below 400 K absorption bands at 295 nm (4.2 eV) and 325 nm (3.8 eV) are formed in addition to the 330-nm band just ascribed to $[X_2^-]$ centers. These bands are illustrated in Fig. 4 for both $c_{\perp}$ and $c_{\parallel}$ crystals with the electric vector of the incident light as indicated on the figure. When unpolarized light is used to measure the absorption in a $c_{\parallel}$ sample an *apparent* reduction in the absorption coefficient of the band compared to that in a $c_{\perp}$ specimen results because of the polarization shown in Fig. 4. In order to facilitate comparison between $c_{\perp}$ and $c_{\parallel}$ crystals a correction factor of 1.35 is used to bring unpolarized measurements on $c_{\perp}$ and $c_{\parallel}$ crystals into agreement. The temperature dependence of the production of defects responsible for these bands is shown in Fig. 5. The curve labeled 10 K should probably be labeled with a higher temperature since the radiation beam heats the crystal. Nonetheless it is interesting that the production efficiency appears to go through a minimum between 145 and 200 K. Figure 6 portrays the thermal annealing of this band and the inset in the figure shows the annealing behavior at low temperatures for a *lightly* irradiated sample containing only a few F centers. The temperature dependence of the width at half-maximum of the band $W(T)$ was also measured. We find $W(10) = 0.72$ eV and $W(300) = 0.92$ eV. The data fit the expression $W(T)^2 = W(10)^2 \coth h\nu_g/2kT$ when $\nu_g = 283$ cm^{-1}. The so-called Huang-Rhys factor[12] can be determined from the expression

$$S = W(10)^2/(h\nu_g)^2 8 \ln 2$$

and is found to be 78. No emission band which can be associated with this absorption has been detected.

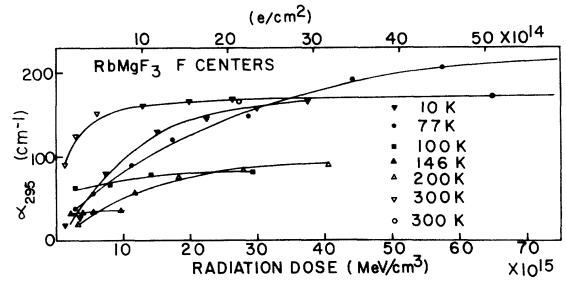

FIG. 5. F-center absorption, α, as a function of absorbed energy for $c_{\perp}$ and $c_{\parallel}$ (open circles) samples irradiated at different temperatures.

C. F_2 centers

When a sample is irradiated at room temperature and annealed or irradiated at 550 K with 1.5-MeV electrons or when a crystal with a previously introduced F band is bleached with 300-nm light at 400 K a series of new bands appear. The room-temperature absorption of a specimen irradiated at 300 K and annealed at 575 K for 30 min is shown in Fig. 7. The bands are polarized with the one at 387 nm (3.2 eV) absorbing light with $\vec{E} \perp \vec{C}$ and the band at 230 nm (5.4 eV) absorbing light with $\vec{E} \parallel \vec{C}$. The 285 nm (4.3 eV) band appears to be at most partially polarized $\vec{E} \perp \vec{C}$. This is verified by the excitation spectrum polarization. An emission band at 430 nm (2.9 eV) is associated with the center responsible for the 387- and 285-nm absorption and is shown in Fig. 8. The excitation spectrum for this emission is shown in Fig. 9 and matches the absorption. The zero-phonon lines for absorption and emission are at the same wavelength.

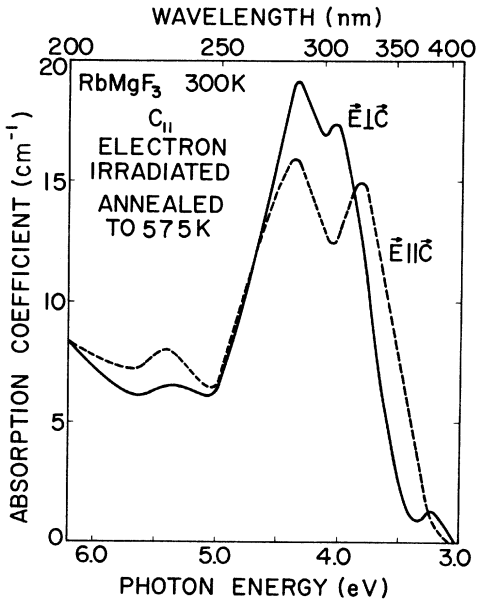

FIG. 7. F_2-center absorption for different $\vec{E}$ polarizations of a crystal irradiated at 300 K and annealed at 575 K for 30 min. Peaks at 310 and 330 nm are due to F centers.

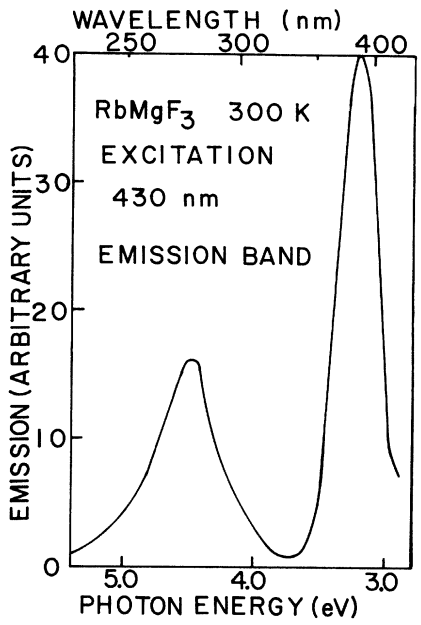

FIG. 9. F_2-center excitation spectrum at 300 K.

The emission decreases markedly about 115 K. The temperature variation of the half-widths W_{em} and W_{abs} are illustrated in Fig. 10. The initial half-widths at 10 K were $W_{em} = 0.173$ eV and $W_{abs} = 0.200$ eV. Analysis of these data yield values of $\nu_g = \nu_e = 180$ cm^{-1} and $S_{abs} = 10$ and $S_{em} = 7$ by area measurements. The calculations of S from half-width data yield $S_{abs} = 14$ and $S_{em} = 10$. A simple linear coupling model for the electron-phonon interaction gives a value $S = (E_{abs} - E_{em})/2h\nu = 7.0$. Table II shows the energy spacing between the sharp lines in emission and absorption for both F_2 and F_3 centers.

As mentioned above the band at 387 nm can be produced by optical bleaching with 300-nm light while the sample is at about 370 K or it can be formed by heat treatment alone. The latter case is illustrated in Fig. 6 which is a plot of the annealing of the optical absorption when the sample is held 10 min at each temperature and then recooled to 300 K. (The open data points are those for a sample irradiated at 300 K and the full data points are those for a crystal irradiated at 550 K initially.)

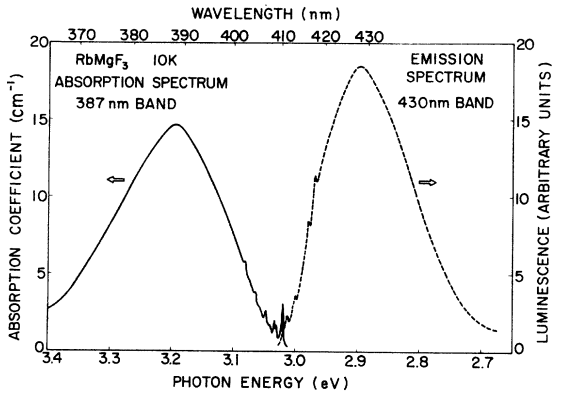

FIG. 8. F_2-center absorption and emission bands in $RbMgF_3$ at 10 K.

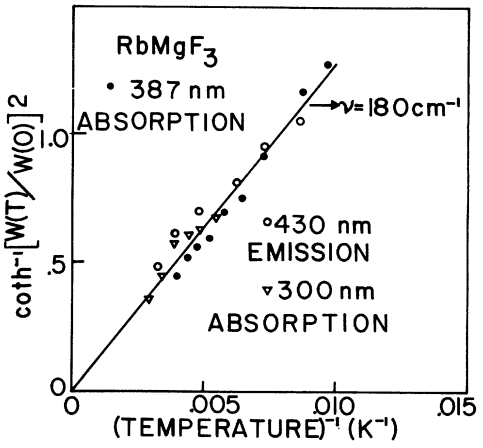

FIG. 10. Temperature dependence of the width at half-maximum, W for F_2 absorption and emission and F_3 absorption.

Table II. Spacing of sharp absorption and emission lines in $RbMgF_3$.

387-nm absorption		430-nm emission	
Peak (eV)	Difference (cm^{-1})	Peak (eV)	Difference (cm^{-1})
3.020		3.019	
3.031	88	3.010	72
3.034	112	2.996	184
3.040	160	2.984	280
3.046	208	2.971	384
3.058	304	2.958	408
300-nm absorption		330-nm emission	
3.966		3.971	
3.974	64	3.960	88
3.976	104	3.948	192
3.988	200	3.936	288
4.000	296	3.922	400
4.010	376	3.911	488
		3.900	576

D. F_3 centers

As can be seen in Fig. 6 when irradiated $RbMgF_3$ specimens are annealed an optical absorption band at 300 nm (4.13 eV) grows in at about 625 K as the F and F_2 centers anneal out. The optical absorption of this band is shown in Fig. 11 along with the emission and the excitation spectra. In the inset the polarization of the band is illustrated for both $\vec{E} \perp \vec{C}$ and $\vec{E} \parallel \vec{C}$. The energy spacings between the sharp lines are shown in Table II. Two emission bands are observed when the crystal is excited with 300-nm light. A band at 330 nm (3.76 eV) is observed at low temperature. At higher temperatures a band at 490 nm (2.53 eV) grows in at the expense of the 330-nm band. The lifetimes at 300 K of both the 330- and the 490-nm emissions are 11 nsec. Both bands are polarized $\vec{E} \perp \vec{C}$. The emission caused by 300-nm excitation at 300 K is shown in Fig. 12. The inset shows the temperature dependence of the intensity of the two bands. A plot of the temperature dependence of the half-width of the absorption band (similar to that for F_2 centers) is shown in Fig. 10 and also yields a value of $\nu_\ell = 180\ cm^{-1}$. The half-width of the 330-nm band changes very little with temperature. Emission from defects is an extremely sensitive measure of their presence. An investigation of the presence of defects after various annealing treatments indicates that the defect responsible for the 387-nm absorption and 430-nm emission is produced by radiation at temperatures as low as 350 K. The defect responsible for the 300-nm absorption and the two emission peaks mentioned above forms around 550 K. Another interesting aspect of these bands is that when only the 300-nm band is present in a crystal and the crystal is then irradiated briefly with electrons or γ rays, the bands attributed to F and F_2 centers grow as the 300-nm band decreases. This is further evidence that we are dealing with F, F_2, and F_3 centers since similar events occur in the well-studied alkali halides.[11]

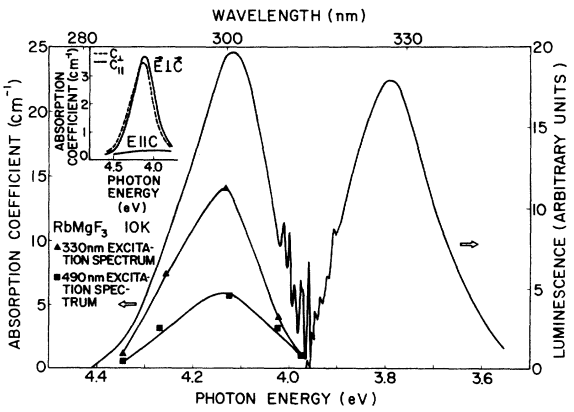

FIG. 11. F_3-center absorption and emission bands at 10 K. Also shown are the excitation spectra for the 330 and 490 nm bands. Inset shows the absorption spectrum of the F_3 center in another sample for different polarizations $\vec{E}$ and orientations $c_\perp$ and $c_\parallel$ of the c axis.

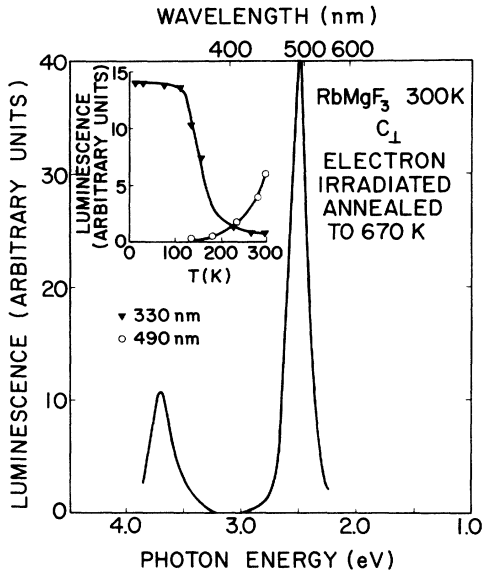

FIG. 12. F_3-center emission at 300 K. Inset shows the temperature dependence of the luminescence.

IV. DISCUSSION

From the polarized absorption data shown in Fig. 2 it is evident that the $[X_2^-]$ centers lie in the basal plane after irradiation at 77 K. The data illustrated in Fig. 3 indicate that these centers become mobile around 90 K, and are then most likely

trapped near impurity ions. They are evidently released from the traps and anneal out about 150 K. Similar behavior has been previously observed for alkali halides and $KMgF_3$.[7,10,13] Two facets of the emission owing to recombination of the electron with the self-trapped hole appear important. First, the x-ray excited emission is not polarized. This would suggest from analogy with alkali halides that the emission is π polarized (one π dipole is in the basal plane and one along the c axis) as would be expected[7,14] or that the centers are created at random in the crystal and rapidly relax, even at 15 K, to a basal plane configuration. The 600-nm emission band seen in Fig. 2 is most likely owing to Mn^{2+}. Mn^{2+} emits 590-nm light in $KMgF_3$.[15] The second aspect of importance in the x-ray excited emission is that although this emission is thermally quenched above 60 K as shown in the inset of Fig. 2, the emission intensity from these centers apparently increases above 90–100 K. Similar effects are observed in $KMgF_3$. In fact, the thermoluminescence of $KMgF_3$ shows a 390-nm peak at 150 K, which could be due to $[X_2^-]$-type centers, that is considerably above the temperature at which the normal $[X_2^-]$ emission is thermally quenched. We suggest that the thermal quenching of the luminescence from *impurity trapped* $[X_2^-]$ centers is markedly different from self-trapped centers and that these trapped centers emit light until they anneal out. This suggestion is in accord with the model proposed by Blair, *et al.*[14] for the $[X_2^-]$ center which takes into account the effect of the next-neighbor cations on the optical transitions.

F centers in this material should have c_{2v} symmetry with three nondegenerate $2p$-type excited states. From the data it would appear that the $2p_x$ and $2p_y$ (basal plane) levels are degenerate. The $2p_z$ level is at a lower energy. The production of stable F centers in this material as a function of temperature is similar to that in MgF_2.[2,3] From the data presented in Fig. 5 it appears that the production efficiency for stable F centers goes through a minimum around 175 K. This defect production behavior has been analyzed by Buckton and Pooley[3] for MgF_2. The interstitials formed during irradiation are evidently mobile enough at higher temperatures that they aggregate to form immobile interstitial clusters. More important Fig. 5 shows that if we use the approximation $nf \simeq 10^{16}\,\alpha_{295}$ where n is the concentration of F centers, f is the oscillator strength, and α_{295} is the F-band absorption coefficient[11] then about 1000 F centers are produced per incident electron. This is far greater than the number expected for elastic collision damage and indicates photochemical processes are responsible for most of the damage.[11] In the case of thermal annealing as the F-center concentration decreases with temperature, F_2 centers are formed and at higher temperatures F_3 centers form. In fact, when a sample initially containing only F centers is annealed to 650 K to form F_3 centers and then reirradiated with γ rays the F_3 centers are destroyed and eventually only the initial F-band absorption, at the same intensity as prior to heat treatment, is observed. When a sample containing F_3 centers is annealed to 850 K most of these centers disappear and a brief γ irradiation does not return the crystal to the original F-center density. The data suggest that the immobile interstitial clusters begin to disintegrate around 850 K, the F center is mobile about 500 K, and either the excited F or the empty negative-ion vacancy moves around 360 K. As can be noted from Fig. 7 some F centers are always present with F_2 centers.

Both F_2 and F_3 centers appear to be aligned in the basal plane hexagon. As illustrated in Fig. 1, three positions exist for the triad of fluorine ions where no Mg^{2+} ions are either above or below the configuration. This configuration should be an ideal low-energy configuration for $[X_2^-]$, F_2, and F_3 centers since no doubly charged ions are nearby. Moreover, defects such as F_2 and F_3 centers will be relatively loosely coupled to the lattice. This is evidenced by the small Stokes shift between absorption and emission and the presence of zero-phonon lines. In Fig. 8 it can be seen that the emission and absorption bands for F_2 centers show almost mirror symmetry about the zero-phonon line. This is the behavior expected from a linearly coupled electron-phonon system and the fact that both ν_g and ν_e are essentially equal suggests that this simple approximation may be valid in this case. We recognize that there are many sophisticated methods of evaluating electron-phonon interactions for color centers.[16] However, in some instances the simple configuration coordinate approach[17,18] can lead to valuable insight and a system in which $\nu_g = \nu_e$ should be ideal for this simple treatment. In this treatment the total energy of the system is plotted on the ordinate and the abscissa specifies the configuration coordinate X. The ground and excited levels are represented by parabolic curves with force constants K_g and K_e. The minima of the lowest two states are separated by an energy E_0 which is related to the zero-phonon energy E_{00} by the expression $E_0 = E_{00} - \frac{1}{2}h\nu_e + \frac{1}{2}h\nu_g$. It is assumed that the primary mode of lattice vibration influencing the defect is a "breathing" mode and that the transitions between the levels are vertical.[17] For the data available on the F_2 center we find

$$E_{abs} = E_0 + \tfrac{1}{2}K_e X_0^2 - \tfrac{1}{2}h\nu_g = 3.20 \text{ eV},$$

$$E_{em} = E_0 - \tfrac{1}{2}K_g X_0^2 + \tfrac{1}{2}h\nu_e = 2.89 \text{ eV},$$

$$E_0 = E_{00} - \tfrac{1}{2}h\nu_e + \tfrac{1}{2}h\nu_g = 3.02 \text{ eV},$$

$$\nu_e = \nu_g = 180 \text{ cm}^{-1} \text{ or } h\nu = 0.022 \text{ eV},$$

$$W_{abs}(10) = (4 \ln 2 h\nu_g / K_g)^{1/2} K_e X_0 = 0.200 \text{ eV},$$

$$W_{em}(10) = (4 \ln 2 h\nu_e / K_e)^{1/2} K_g X_0 = 0.173 \text{ eV}.$$

If we assume a mass for the ground state of 4×10^{-22} g then $X_0 = 0.11$ Å, $K_g = 29$ eV/Å^2, and $K_e = 32$ eV/Å^2. The consistency of this approach can now be checked by comparing the S values derived from the expression $S_{abs} h\nu = \frac{1}{2} K_e X_0^2$. From this expression we find $S_{abs} = 8.8$ and $S_{em} = 8.0$. This is essentially in agreement with the measured values and suggests that in some cases the simple configurational coordinate approach can be helpful. The discrepancy in S values obtained from half-width and area measurements probably arises from nonlinear coupling to phonons. The intensity of the emission at 430 nm changes rapidly with temperature so that the area under the emission band is decreased at temperatures above 120 K. This could indicate a thermal quenching of the emission, but from the simple analysis given above this is not likely. More likely, this decrease is a transfer from the singlet excited state to the lower triplet state where thermal quenching could occur as discussed by Wood and Meyer.[19]

The F_3 center has been studied in detail by Silsbee.[20] From stress experiments and the H_3 molecule work of Hirschfelder[21] he was able to establish the energy-level sequence in KCl. We find two emission bands from the F_3 center in $RbMgF_3$ both of which are polarized with $\vec{E} \perp \vec{C}$. This suggests that transitions from the $^2A_1$ and $^2A_2$ levels go to the ^2E ground state.[20,22] Such an assignment is in accord with Silsbee's investigation. The half-width of the 330-nm emission band remains essentially constant from 10 K to at least 200 K. This means that the excited electronic state in a configuration coordinate diagram would be relatively flat. The thermal growth of the 490-nm emission band indicates the level responsible for this band is only slightly higher in its relaxed excited state than the level giving rise to the 330-nm emission. Moreover, the fast lifetime of the 490-nm emission suggests it is an allowed transition.

The spacing of the sharp absorption and emission lines for the F_2 and F_3 bands indicates that a number of low-lying lattice modes interact with these defects. Since little or no infrared or Raman data much less neutron scattering data are available on $RbMgF_3$ it is not possible at this time to make an analysis of the electron-phonon interactions in these crystals. It is interesting, however, that the splittings are similar for absorption and emission of the two types of centers. This suggests that the ground and excited states of these two defects interact with the same phonon modes.

V. SUMMARY

The primary purpose of this paper is to determine whether photochemical or elastic collision damage is prevalent in $RbMgF_3$ and to make tentative identification of the radiation-induced defects. As discussed, the fact that about 1000 F centers are formed per incident electron strongly suggests the photochemical damage process is dominant. We have been able to identify the optical transitions associated with X_2^-, F, F_2, and F_3 centers. Perhaps most important is the finding that vacancies do not aggregate during irradiation at 300 K in this material.

ACKNOWLEDGMENTS

We are indebted to Y. Chen, E. Sonder, and F. Sherrill of Oak Ridge National Laboratory for the impurity and x-ray analyses of one sample. Also we appreciate the help of J. J. Martin on crystal growth and R. C. Powell and G. Venikouas on the lifetime measurements.

---

†Supported by NSF Grant No. DMR 73-02439 A01.

[1] *Crystals With the Fluorite Structure*, edited by W. Hayes (Oxford, Clarendon 1974); P. J. Call, W. Hayes, J. P. Stott, and A. E. Hughes, J. Phys. C 7, 2417 (1974).

[2] W. A. Sibley and O. E. Facey, Phys. Rev. 174, 1076 (1968).

[3] M. R. Buckton and D. Pooley, J. Phys. C 5, 1553 (1972).

[4] C. R. Riley and W. A. Sibley, Phys. Rev. B 1, 2789 (1970).

[5] N. S. Altshuler, B. N. Kazakov, S. L. Korableva, L. D. Livanova, and A. L. Stolor, Opt. Spektrosk. 33(2), 207 (1972).

[6] J. J. Rousseau, M. Binois and J. C. Fayet, C. R. Acad. Sci. B 277, 617 (1973).

[7] R. Alcala, N. Koumvakalis, and W. A. Sibley, Phys. Status Solidi A 30, 449 (1975).

[8] R. D. Burbank and H. T. Evans, Jr., Acta Crystallogr. 1, 339 (1948).

[9] M. W. Shafer and T. R. McGuire, J. Phys. Chem. Solids 30, 1989 (1969).

[10] M. N. Kabler, in *Point Defects in Solids*, edited by J. H. Crawford and L. M. Slifkin (Plenum, New York, 1972), Vol. I, p. 327.

[11] E. Sonder and W. A. Sibley, in Ref. 10, p. 201.

[12] D. B. Fitchen, in *Physics of Color Centers*, edited by W. B. Fowler (Academic New York, 1968), p. 293.

[13] M. Ikeya and J. H. Crawford, 1974 Conference on Color Centers in Ionic Crystals, Sendai, Japan; Phys. Lett. A 45, 213 (1973).

[14] I. M. Blair, D. Pooley, and D. Smith, J. Phys. C 5, 1537 (1972).

[15] S. Yun, K. H. Lee, W. A. Sibley, and W. E. Vehse,

Phys. Rev. B 10, 1665 (1974).
[16]M. Möstoller, B. N. Ganguly, and R. F. Wood, Phys. Rev. B 4, 2015 (1971).
[17]C. C. Klick, D. A. Patterson, and R. S. Knox, Phys. Rev. 133, A 1717 (1964).
[18]J. J. Markham, in *Solid State Physics Supp.* 8, edited by F. Seitz and D. Turnbull (Academic, New York, 1966).
[19]R. F. Wood and A. Meyer, Solid State Commun. 2, 225 (1964); R. F. Wood, Phys. Rev. 151, 629 (1966).
[20]R. H. Silsbee, Phys. Rev. 138, A180 (1965).
[21]J. O. Hirshfelder, J. Chem. Phys. 6, 795 (1938).
[22]A. M. Stoneham, *Theory of Defects in Solids* (Clarendon, Oxford, 1975).

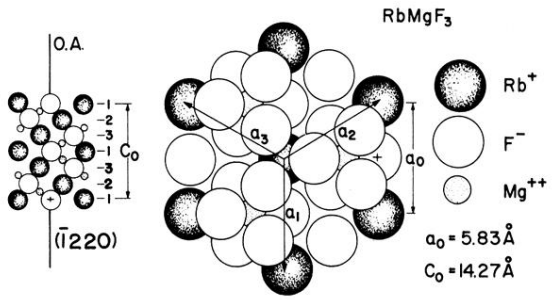

FIG. 1. $RbMgF_3$ model. Shown are the basal plane (three layers with 7 Rb^+ ions, and 12 F^- ions in the first layer and 3 Mg^{2+} ions in the second) and the close-packed sequence of ions along the optic axis which lie in the $(\bar{1}220)$ plane.